EVALUATION OF THE MATERIAL PROPERTY AND SEISMIC PERFORMANCE OF A ROCKFILL DAM DURING LARGE DOUBLET EARTHQUAKES

Nario YASUDA[1], Zengyan CAO[2] and Kosuke NAKAMORI[3]

[1]Member of JSCE, Eng. Division 1, Japan Dam Engineering Center (JDEC)
(2-9-7 Ikenohata, Taito-ku, Tokyo 110-0008, Japan)
E-mail: yasuda@jdec.or.jp (Corresponding Author)
[2]Member of JSCE, J-POWER Business Service Corporation (4-6-4, Tsukiji, Chuo-ku, Tokyo 104-0045, Japan)
E-mail: sou@jpbs.co.jp
[3]Member of JSCE, Department of Prefectural Land Development, Mie Prefecture
(Komie 13, Tsu-city, Mie 514-8570. Japan)
E-mail: nakamk27@pref.mie.lg.jp

The relationship between the shear modulus and shear strain of embankment materials is evaluated based on earthquake records. When the average shear strain of a dam body is less than approximately 2.0×10^{-4}, the decreased stiffness of the embankment materials can be promptly recovered. However, when the shear strain exceeds 1.0×10^{-3}, one week or more may be necessary for the stiffness to be recovered. Using the evaluated nonlinear properties, the behaviors of the Aratozawa dam during an assumed large doublet earthquake are investigated through numerical analyses. The results indicate that the change in the dynamic characteristics of the dam in response to the first event considerably influences the dynamic behaviors of the dam during the second event. In addition, a procedure to evaluate the seismic performance of rockfill dams during doublet earthquakes is proposed. In this approach, the variation in the material properties in the first and second events is considered. The final residual subsidence of the dam is predicted by summing the sliding displacements caused by each earthquake and subsidence related to the shaking and rearrangement of soil particles. Furthermore, as a precautionary measure for assumed large doublet earthquakes, after a dam experiences a large earthquake, it is recommended that the reservoir be adjusted to a safe water level and maintained at that level for at least one week as an emergency response measure.

Key Words : *rockfill dam, dynamic behavior, seismic performance evaluation, doublet earthquake*

1. INTRODUCTION

In Japan, the seismic performance evaluation of existing dams during large earthquakes (maximum design earthquakes[1)]) is conducted by performing dynamic response analyses. In the dynamic response analysis and seismic performance evaluation of these dams, engineers consider the normal operating conditions of the dams as the initial conditions for the analysis and assume the dam to be subjected to a single earthquake. However, after the Iwate-Miyagi Nairiku Earthquake in 2008 (M_j 7.2, where M_j is the Japan Meteorological Agency (JMA) magnitude scale), the dynamic characteristics of the Aratozawa dam, a 74.4 m high rockfill dam located approximately 15 km from the epicenter, deteriorated considerably[2), 3),4)]. Approximately one week after the main shock, the natural frequencies of the dam were found to be nearly recovered. This phenomenon has not yet been reported in dam engineering. Furthermore, during the 2016 Kumamoto earthquake (M_j 6.5 and 7.3 on April 14 and 16, respectively), Mashiki town experienced ground motions of JMA seismic intensity VII two times within 28 h[5)]. Based on these facts, it is reasonable to assume that in the future, a dam may experience multiple large seismic events in a short period. Such situations have not been addressed in the current "Guidelines of the Seismic Performance Evaluation of Dams for Large-Scale Earthquakes (draft)" [6)]. Thus, it is significant in the context of dam engineering to clarify the behaviors of rockfill dams subjected to multiple earthquakes and establish a method to address this issue. In this study, the behavior of the Aratozawa dam subjected to ground motions of JMA seismic intensity VII, before the corresponding dynamic characteristics fully recover from the state after the Iwate-Miyagi Nairiku Earthquake in 2008, is examined. Further-

more, to realize dam management during earthquakes, appropriate emergency measures must be established to suitably respond to large doublet earthquakes. The dynamic response analysis and seismic performance evaluation methodologies of rockfill dams subjected to large doublet earthquakes have emerged as key research subjects in dam safety management. Thus, this study clarifies the behavior of a rockfill dam subjected to a large doublet earthquake and proposes a seismic performance evaluation method and emergency response measures in preparation for the occurrence of large doublet earthquakes in the future.

In this study, the responses of the Aratozawa dam to two large earthquakes ("Earthquake A": the Iwate-Miyagi Nairiku Earthquake in 2008; "Earthquake B": a synthetic local earthquake) are analyzed. The dynamic response analyses of the dam are performed considering the variation in the dynamic characteristics and material properties of the dam during each earthquake. The sliding deformation and deformation related to the shaking and rearrangement of soil particles (a phenomenon in which the volume shrinks as the soil particle arrangement changes due to vibrations) are calculated considering the change in the material properties of the dam. The final residual deformation of the dam after the doublet earthquake is predicted by summing the deformations induced by each earthquake. Moreover, the seismic safety of the dam is verified considering the residual deformation. In addition, in preparation for large doublet earthquakes, emergency response measures are recommended for rockfill dams subjected to large earthquakes.

2. EVALUATION OF NONLINEAR MATERIAL PROPERTIES BY ANALYZING EARTHQUAKE RECORDS

(1) Dam specifications

The Aratozawa dam is a 74.4 m high rockfill dam with a central clay core in the Kitakami river, Kurihara city, Miyagi prefecture. **Table 1** summarizes the main features of the dam. The location, plan view, and standard cross-section of the dam and the locations of seismographs are shown in **Fig. 1**. Notably, seismographs with three components (perpendicular to the dam axis, parallel to the dam axis, and vertical directions) are installed at the dam base (F), mid-height of the core (M), and dam crest (T).

(2) Evaluation of nonlinear properties by considering earthquake records

Since 1992, immediately after the dam body completion, many earthquakes have been recorded.

Table 1 Main features of the Aratozawa dam.

Dam location	Kurihara City, Miyagi Prefecture
Dam type	Rockfill dam with central clay core
Dam height	74.4 m
Crest length	413.7 m
Crest width	10.0 m
Crest elevation	EL. 279.4 m
Slope gradient	Upstream: 1:2.7 Downstream: 1:2.1
Embankment volume	3,048,000 m^3
Basin area	20.4 km^2
Total water volume	13,850,000 m^3
Design seismic coefficient	0.15 (dam body), 0.18 (intake tower, bridges), 0.16 (spillway)

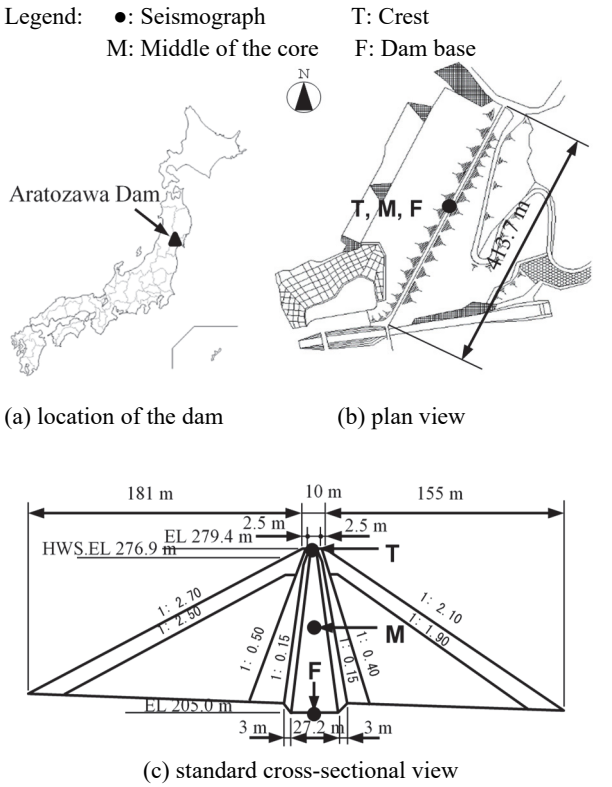

Fig. 1 Location, plan view, and standard cross-section of the dam and locations of the seismographs.

Among these earthquakes, approximately 500 and 37 earthquakes were recorded with a maximum acceleration of over 10 cm/s^2 and 100 cm/s^2 at the dam base (F), respectively. On June 14, 2008, the Iwate-Miyagi Nairiku Earthquake (M_j 7.2) occurred. At the Aratozawa dam, located approximately 15 km from the epicenter, a maximum acceleration of 1024 cm/s^2 in the direction perpendicular to the dam axis was recorded at the dam base. This earthquake corresponds to the highest intensity earthquake ever recorded at the base of a dam in Japan. During the

earthquake, the natural frequency and acceleration amplification factor of the dam sharply decreased. For example, in the direction perpendicular to the dam axis, the fundamental frequency of the dam decreased from 3.2 Hz to 2.2 Hz. Approximately one week after the main shock, the natural frequencies of the dam nearly fully recovered to their pre-earthquake values. The mechanism of this variation has been discussed to a certain extent in a previous study[2]. Furthermore, many small aftershocks occurred after the main shock. It is presumed that the material particles loosened by the main shock were promoted to mesh by the micro vibration of the aftershocks, and the recovery of the shear modulus of the embankment material was accelerated. However, there are insufficient data to explain the contributions of other factors, such as creep and material relaxation. Therefore, the detailed recovery mechanism of the shear modulus requires further investigation.

A decrease in the natural frequency of the dam corresponds to a reduction in the stiffness of the embankment materials. The relationship between the shear modulus G and fundamental frequency f_1 is shown in Equation (1).

$$\frac{f_1^2}{f_{10}^2} = \frac{G}{G_0} \tag{1}$$

Here, G_0 and f_{10} denote the initial shear modulus of the material under a small strain and initial fundamental frequency of the dam, respectively. Therefore, the rate of change in the shear modulus of the materials can be obtained from the rate of change in the fundamental frequency of the dam by using Equation (1) [7]. In addition, the transfer function of the dam can be obtained by analyzing the earthquake records at the crest of the dam (T) and dam base (F), and the frequency corresponding to the first peak of the transfer function can be regarded as the fundamental frequency of the dam. An example is shown in **Fig. 2**. According to the analysis of the records of past small earthquakes, the fundamental frequency of the Aratozawa dam can be calculated as 3.2 Hz [2]. To obtain the fundamental frequency f_1 of the dam during each earthquake, earthquake records of different acceleration amplitudes are selected, focusing on the Iwate-Miyagi Nairiku Earthquake in 2008 and its aftershocks. The selected earthquake records are listed in **Table 2**. These earthquake records (Nos. 1–20) are numbered in the order of occurrence. On the other hand, by integrating the acceleration records obtained at the crest and dam base, the relative displacement of the dam body is calculated. Furthermore, by dividing the relative displacement by the dam height, the average shear strain γ_{ave} of the dam can be obtained.

Table 2 Earthquake records and obtained results.

No.	Time of occurrence	M	A_{max} ※1 (cm/s^2)	f_1 ※2 (Hz)	γ_{ave} ※3 (10^{-5})
1	1996/08/11 03:12	6.1	28	2.93	5.32
2	1996/08/11 08:10	5.8	36	2.83	3.92
3	1996/08/11 15:01	4.9	30	3.03	0.66
4	2003/05/26 18:24	7.1	114	2.64	17.27
5	2008/06/14 08:43	7.2	1024	1.51	156.6
6	2008/06/14 09:00	4.2	99	2.34	0.37
7	2008/06/14 09:01	4.0	482	1.95	7.76
8	2008/06/14 09:14	3.6	151	2.25	1.66
9	2008/06/14 09:20	5.7	76	2.05	7.98
10	2008/06/14 10:40	4.8	120	2.15	5.96
11	2008/06/14 12:09	4.1	92	2.25	2.84
12	2008/06/14 12:10	4.8	79	2.34	2.48
13	2008/06/14 19:11	4.1	229	2.15	5.17
14	2008/06/16 23:14	5.3	76	2.25	3.76
15	2008/06/21 12:19	2.8	9	3.03	0.17
16	2008/07/24 00:26	6.8	27	2.60	6.53
17	2008/09/25 15:04	4.1	119	2.54	7.00
18	2011/03/11 14:46	9.0	102	2.31	18.58
19	2011/04/07 23:32	7.2	120	2.34	24.05
20	2015/05/1306:13	6.8	18	2.94	1.35

Note: ※1 Maximum value of the three directional components of the dam base (F)

※2 Frequency corresponding to the first peak of the transfer function obtained from the earthquake records

※3 Average shear strain obtained from the relative displacement determined by integrating the acceleration records of earthquakes

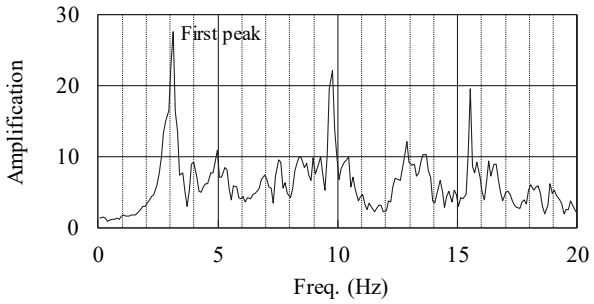

Fig. 2 Sample transfer function obtained from earthquake records.

From each earthquake record, the fundamental frequency of the dam in the direction perpendicular to the dam axis and average shear strain are calculated and summarized, as shown in **Table 2**. The value of G/G_0 is calculated according to Equation (1) and plotted with the average shear strain γ_{ave} in **Fig. 3**. In **Fig. 3**, the results obtained from the earthquake records at the crest and the middle of the core are indicated by ● and ○, respectively. It is obvious that the results based on the earthquake records at different elevations are approximately the same. The results based on the earthquake records at the crest are numbered 1 – 20 in the figure, which will be

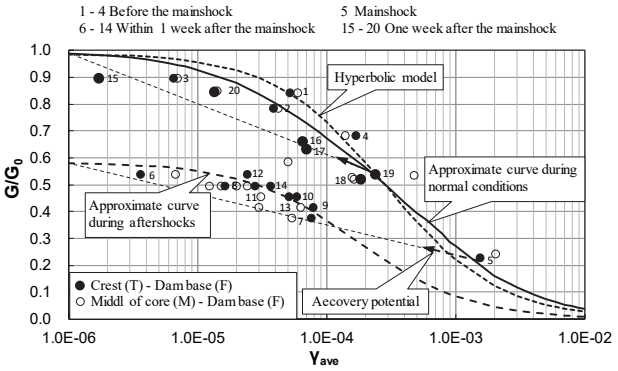

Fig. 3 G/G_0-γ relationship obtained from earthquake records.

used in the subsequent studies. The figure indicates that the decreased stiffness of the embankment materials is immediately recoverable when the average shear strain γ_{ave} caused by an earthquake is less than approximately 2.4×10^{-4} (the value corresponding to earthquake 19 in **Table 2**). The stiffness may recover with the potential indicated by the solid arrow in the figure. However, when γ_{ave} exceeds 15.7×10^{-4} (the value corresponding to earthquake 5 in **Table 2**), the decreased stiffness recovers at different potentials indicated by the dashed arrow. Therefore, it is presumed that there exists a limit value of the shear strain between the abovementioned two values. Shear strain can be recovered when it is less than the limit value. Furthermore, the knowledge obtained from this case and limit value of the recoverable shear strain are applicable for other rockfill dams. It is noted that G_0 can recover to only 58% of its original value. Based on the $G/G_0-\gamma_{\mathrm{ave}}$ relationship and the occurrence time of the earthquakes, the seismicity can be divided into the following three periods:

Period I. Earthquake 1 to earthquake 5
Period II. Earthquake 6 to earthquake 14
Period III. Earthquake 15 to earthquake 20

The $G/G_0-\gamma_{\mathrm{ave}}$ relationship in Period I can be approximated by a curve (solid line), which is in close agreement with the normal hyperbolic model represented by the dashed line in the same figure. However, this relationship is considerably different from that in the aftershock period (Period II). In response to the Iwate-Miyagi Nairiku Earthquake in 2008 (No. 5), the material properties of the Aratozawa dam significantly changed, although temporarily. Thus, in the earthquake response analysis and seismic performance evaluation of the dam in Period II, the dynamic characteristics and material properties of the dam during this period must be considered instead of the initial conditions. In addition, the $G/G_0-\gamma_{\mathrm{ave}}$ relationship in Period III can be estimated to have nearly recovered to the relationship exhibited in Period I. Although the mechanism of the stiffness recovery cannot be concretely described, the consolidation effect of the loosened coarse-grained material is the primary reason. Approximately one week was required for the recovery to occur for the rockfill dam, which is a large soil structure. The shear strain corresponding to $G/G_0=0.5$ is 2.9×10^{-4} is similar to the reference shear strain (3.0×10^{-4}) determined by conducting a reproduction analysis of a past earthquake experienced by the Aratozawa dam[3]. In Period II, no data corresponding to a shear strain of 10^{-4} or more are present; however, when the existing data are fitted with a hyperbola, the relationship represented by the dotted line is obtained. These nonlinear characteristics are considered in the subsequent seismic response analyses of the dam.

3. EVENTS CONSIDERED AND STUDY METHODS

(1) Events considered

In this study, the terms "Earthquake A" and "Earthquake B" are used instead of "foreshock" and "main shock," respectively. For the Aratozawa dam, the Iwate-Miyagi Nairiku Earthquake in 2008 is considered Earthquake A in the following analysis. Before the dynamic characteristics of the dam recover, an earthquake of M_j 6.5 (Earthquake B) is assumed to occur directly underneath the dam. The seismic behaviors of the Aratozawa dam subjected to such a large doublet earthquake are predicted, and the dam safety is evaluated considering the analysis results. In addition, the possibility of liquefaction of the dam and foundation must be determined according to the evaluation guidelines pertaining to embankment dams. However, since the Aratozawa dam is a rockfill dam constructed using modern technology, the risk of liquefaction is extremely low; thus, the liquefaction is not discussed in this paper.

The acceleration records obtained at the dam base (F) in Earthquake A are considered to generate the input ground motions. For Earthquake B, artificial seismic waves are generated considering the earthquake records obtained at the dam base during the aftershocks that occur immediately after Earthquake A. The ground motions are created by fitting the acceleration records to the lower limit spectra defined in the evaluation guidelines of dams during large earthquakes[6], assumed to be equivalent to an M_j 6.5 earthquake.

(2) Study methods

The earthquake responses of the dam are analyzed using the equivalent linearization method, which is a commonly available analysis method, instead of the sequential nonlinear analysis technique. The main

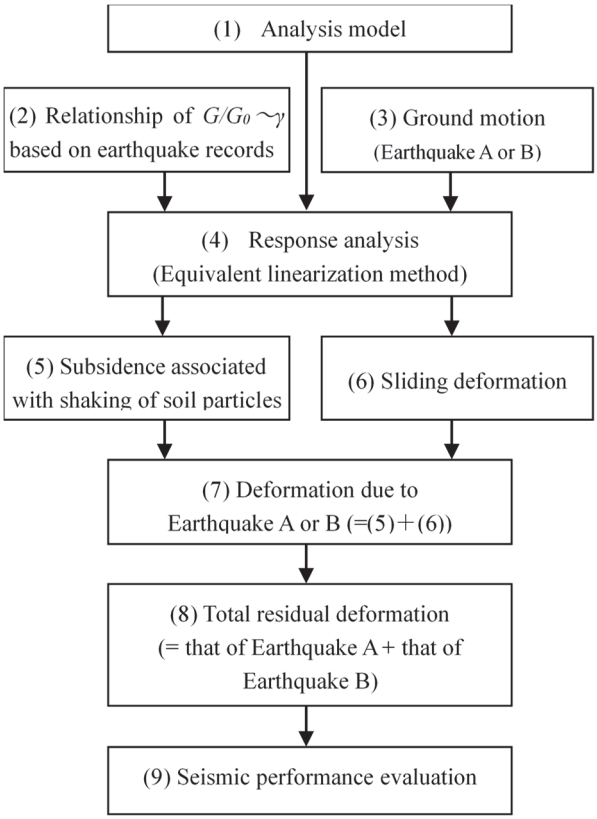

Fig. 4 Procedure of the response analysis and performance evaluation of rockfill dams subjected to large doublet earthquakes.

factors influencing the seismic behavior and seismic safety evaluation of dams include the ground motion, material properties such as strength and elastic modulus, and reservoir conditions. If the material properties of the dam change due to Earthquake A, the variation should be considered when analyzing the response of the dam to Earthquake B. As shown in **Fig. 3**, the initial shear modulus and $G/G_0 - \gamma_{ave}$ relationship in Period II are considerably different from those in the other periods. Therefore, to predict the earthquake responses of the dam to Earthquake B in approximately one week after Earthquake A, the initial shear modulus G_0 and $G/G_0 - \gamma_{ave}$ relationship of the materials during this period are considered.

The residual deformation of the dam due to the doublet earthquake is predicted by summing the deformations calculated separately for each event. The deformation includes the sliding component and subsidence associated with soil particle oscillation. **Figure 4** shows the procedure of the earthquake response analysis and seismic performance evaluation for rockfill dams subjected to the considered large doublet earthquake. The material properties (i.e., step [2] in **Fig. 4**) considered in the analyses of the two events are different.

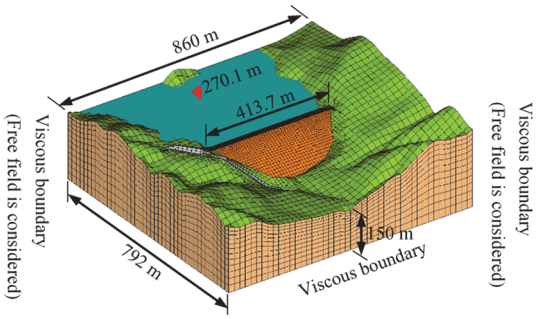

Fig. 5 Analysis model.

4. RESPONSE OF THE DAM TO EARTHQUAKE A

(1) Reproduction analysis

Figure 5 shows the 3D analysis model of the dam–reservoir–foundation system. The earthquake response analysis program "UNIVERSE" [8] is used for the analysis. Considering the influence of the vibration of the free fields outside the analysis model, viscous boundary conditions[9] are applied at the perimeter and bottom boundaries of the foundation rock. In the static stress analysis before the earthquake, the influence of the reservoir water on the water level (EL 270.1 m) during the earthquake and that of the pore water pressure inside the dam are considered. However, the influence of the hydrodynamic pressure and excessive pore water pressure are neglected in the earthquake response analysis since the interaction between the embankment material and reservoir water is not yet fully understood.

A strong nonlinearity likely occurred in the dam during Earthquake A. However, the equivalent linearization method is used in this study as it is a generally feasible analysis method to consider the influence of nonlinear material properties. The initial shear moduli of the embankment materials are set according to Sawada's equation[10], which is based on the compressional and shear wave logging (P-S logging) of several rockfill dams. To enhance the accuracy of the initial shear moduli, the values are slightly adjusted to ensure that the fundamental frequencies of the dam obtained from eigenvalue analysis are consistent with the results estimated from past small earthquakes. The approximate curve in the normal state (solid line) shown in **Fig. 3** is used to consider the shear strain dependence of the shear moduli of the embankment materials.

The damping is evaluated as the Rayleigh damping proportional to the mass and stiffness, and the damping ratio h is determined using Equation (2).

Table 3 Damping ratios determined through the reproduction analysis of the past earthquakes[3].

Classification[*1]	Max. damping ratio h_{max}	Init. damping ratio h_0
A: lower part of the core	20%	5%
B: upper part of the core	30%	
C: filter D: transition	30%	
E: rock (inner) F: rock (outer)	20%	

Note: ※1 Classifications A, B, etc. are shown in **Fig. 6**.

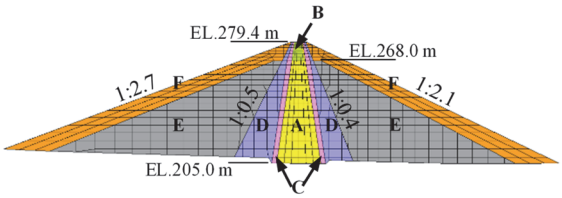

Fig. 6 Zoning of the materials.

$$h = h_{\max}\frac{\gamma}{\gamma + \gamma_r} + h_0 \qquad (2)$$

where h, h_0, and $h_{\max}$ denote the damping ratio, its initial value (in the range of small strain), and its maximum value, respectively. The values of h_0 and $h_{\max}$ listed in **Table 3** and **Fig. 6** are determined through the reproduction analysis of the dynamic behavior of the dam during past earthquakes[3]. Value γ is the effective shear strain (2/3 of the maximum value obtained in the previous iteration of the calculation). Value γ_r is the reference shear strain, which can be determined from **Fig. 3** to be 2.9×10^{-4} when G/G_0 = 0.5. Poisson's ratios of the embankment materials are set according to Sawada's equation[10]. The densities of the embankment materials, foundation rock, and spillway concrete, as determined from the construction quality control tests of the dam (listed in **Table 4**), are used.

Spillway concrete is treated as a linear material with an elastic modulus of 30000 N/mm^2 and a Poisson's ratio of 0.2. Furthermore, the foundation rock is modeled as a linear material. The shear modulus of this rock is 5500 N/mm^2, determined through conversion from the average shear wave velocity of the rock (V_s = 1440 m/s). The Poisson's ratio of the foundation rock is 0.25, which is estimated to be the average value for the rock.

In terms of the input ground motions, since Earthquake A is a real earthquake, the input ground motions at the bottom boundary of the model (as shown in **Fig. 5**) are generated by performing the inverse analysis of the earthquake records at the dam base (F).

As an example of the earthquake responses of the dam, **Fig. 7** shows the acceleration response histories of the dam crest (T). Although a certain difference exists in the maximum acceleration values between the analysis results and earthquake records, the response waveforms are generally coincident. A high reproducibility is obtained in the acceleration response histories, except for the period from 5.4 s to 6.8 s in the direction perpendicular to the dam axis. Furthermore, the waveforms from 0 s to 4 s in the acceleration response histories have approximately the same phase, or the peak values pertaining to the earthquake records appear slightly earlier than those of the analysis results. In contrast, in the waveforms after 4 s, the peak values pertaining to the earthquake records appear slightly later than those of the analysis results. This phenomenon likely occurs because in the equivalent linearization method, the stiffness of the embankment materials is a constant for the whole history; however, in the actual dam, the rigidity of the dam decreased after the principal motion of the earthquake, which resulted in decelerated wave propagation. **Figure 8** shows the comparison of the Fourier spectra of the acceleration responses at the dam crest. This figure shows that the behavior of the dam during Earthquake A can be effectively reproduced.

Table 4 Density of the materials considered in the analysis.

Classification		Density (g/cm^3)	
		Wet	Saturated
Core		2.04	2.10
Filter		2.34	2.43
Transition		2.24	2.33
Upstream rock	Inner	2.15	2.29
	Outer	2.15	2.32
Downstream rock	Inner	2.18	2.32
	Outer	2.13	2.30
Spillway concrete		2.40	
Bedrock		2.60	

(2) Residual deformation caused by Earthquake A

The seismic performance of rockfill dams is evaluated considering the residual deformation under the current guidelines[6]. As described in the previous section, the seismic behavior of the Aratozawa dam in response to Earthquake A is reproduced through a numerical analysis. Using the analysis results, the residual deformation of the dam caused by Earthquake A can be calculated.

The residual deformation of the dam caused by the earthquake is calculated using two methods corresponding to the two simultaneous deformation mechanisms: sliding and subsidence. To consider the deformation due to sliding, the method proposed by Watanabe and Baba[12] is used, which is based on the

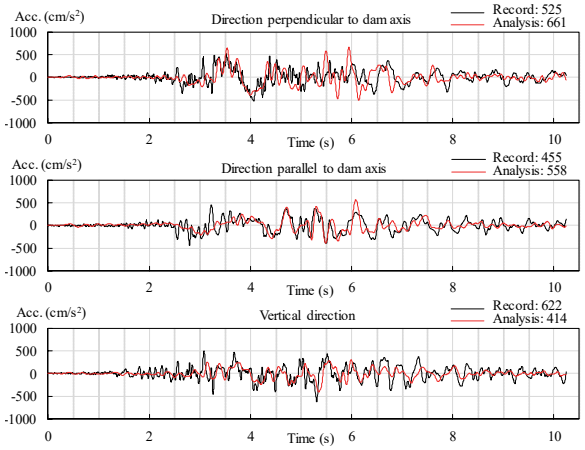

Fig. 7 Acceleration response determined by the reproduction analysis and earthquake records at the dam crest.

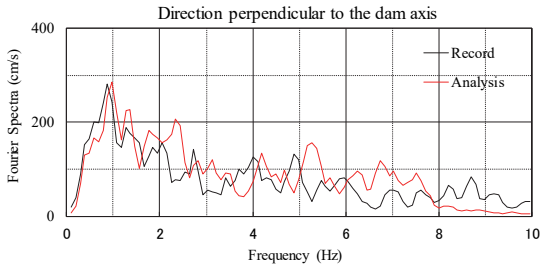

Fig. 8 Fourier spectra and transfer function of the acceleration response at the dam crest.

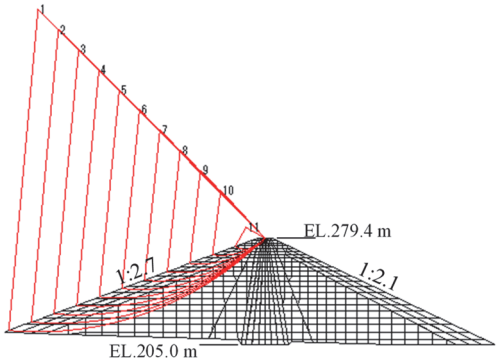

Fig. 9 Sample sliding arcs.

Table 5 Strength parameters of the embankment materials used in the sliding deformation calculation[11].

Division		Cohesion (MPa)	Friction angle (°)	Evidence
Core		0.049	33.2	Based on triaxial compression tests
Filter		0.078	42.2	
Transition		0.039	39.9	
Upstream rock	Inner	0.049	42.7	
	Outer		43.4	
Downstream rock	Inner		40.2	
	Outer		42.7	

sliding block assumption and use of the acceleration and stress results of the earthquake response analysis. In general, 3D sliding calculations have not yet been applied; therefore, a 2D calculation is performed using the standard cross-section extracted from the 3D model shown in **Fig. 5**. In total, 1235 arcs are established, covering all the possible sliding zones. **Figure 9** shows an example of the arcs with the upper end at the center of the crest. To fully investigate the stability of the dam, the arcs sliding toward the upstream side are divided into three groups. The arcs for which both ends pass through only the upstream surface of the dam are referred to as the "U1 Group." The arcs for which the upper and lower ends lie at the crest and upstream surface are categorized to be in the "U2 Group." In addition, the arcs that cut the core zone correspond to the "U3 Group." Similarly, the arcs sliding downstream are divided into the "D1 Group," "D2 Group," and "D3 Group." **Table 5** shows the strength parameters of the embankment materials based on the results of material tests during dam construction.

Except for one arc each near the upstream and downstream toes of the dam, the safety factors of all the other arcs are greater than 1. The minimum sliding safety factor is 0.847; however, nearly no sliding displacement occurs in the sliding analysis (the maximum value is 0.04 cm). This result suggests that sliding in the Aratozawa dam did not occur during Earthquake A (the Iwate-Miyagi Nairiku Earthquake in 2008). This result is consistent with the field survey[13] after the earthquake, which reported that no sliding phenomenon due to the earthquake was observed.

In addition to sliding, subsidence may be caused by the shaking and rearrangement of the soil particles in earthfill dams due to strong earthquakes[14]. Such deformation can be attributed to the decrease in the rigidity of the dam. The subsidence can be conveniently evaluated by calculating the deformation due to the dead load by using the shear moduli of the embankment materials before and after the earthquake[15]. The rigidities of the embankment materials before Earthquake A are evaluated considering the initial shear moduli used in the earthquake response analysis, and those after the earthquake are evaluated for each element considering the converged shear moduli during Earthquake A with the equivalent linearization method. The 3D model shown in **Fig. 5** is used for this analysis. The difference in the deformations before and after the earthquake can be regarded as the residual deformation caused by the earthquake. Specifically,

$$U_r = U_a - U_b \tag{3}$$

where $U_r$is the residual deformation caused by the earthquake, and U_b and U_a denote the deformations

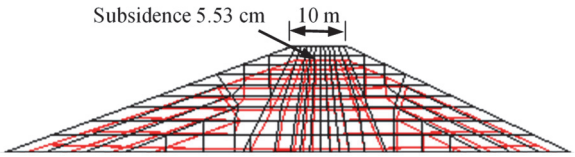

Fig. 10 Deformation near the crest caused by Earthquake A.

due to the dead load before and after the earthquake, respectively.

It is observed that the maximum subsidence of 5.53 cm occurs at the crest. The deformation near the crest is shown in **Fig. 10**. Since the core zone and rock zone are continuous in the analysis model, a smooth deformation is calculated. However, the amount of subsidence of the core zone is larger than that of the rock zone. Since no sliding behavior was observed during Earthquake A, the residual deformation of the dam caused by Earthquake A equals that related to the shaking and rearrangement of soil particles, with a maximum value of 5.53 cm at the crest of the dam. According to the field survey[13] after Earthquake A, the subsidence at the crest of the Aratozawa dam was approximately 20 cm. However, since the survey was conducted 16 d after the mainshock, the measured subsidence includes the contributions of many aftershocks and the increment from half a year ago (since December 4, 2007). Therefore, the exact residual deformation caused by Earthquake A itself cannot be confirmed. Nevertheless, the calculated maximum subsidence can be considered to be consistent with that of the measured subsidence.

5. RESPONSE OF THE DAM TO EARTHQUAKE B

(1) Response analysis

Using the same model shown in **Fig. 5** and the material properties exhibited after Earthquake A, the response of the Aratozawa dam to Earthquake B is analyzed. In the analysis, the equivalent linearization method is used for the same reason mentioned in the analysis of Earthquake A, although a stronger nonlinearity of the embankment materials is considered to occur in Earthquake B.

As shown in **Fig. 3**, after Earthquake A, the shear moduli of the embankment materials dropped to approximately 58% of those before Earthquake A ($G/G_0 = 0.58$ corresponding to a shear strain of 10^{-6}) for approximately one week. To consider the nonlinearity of the materials, earthquake response analysis is performed considering the approximate curve during the aftershocks, as shown in **Fig. 3**. The

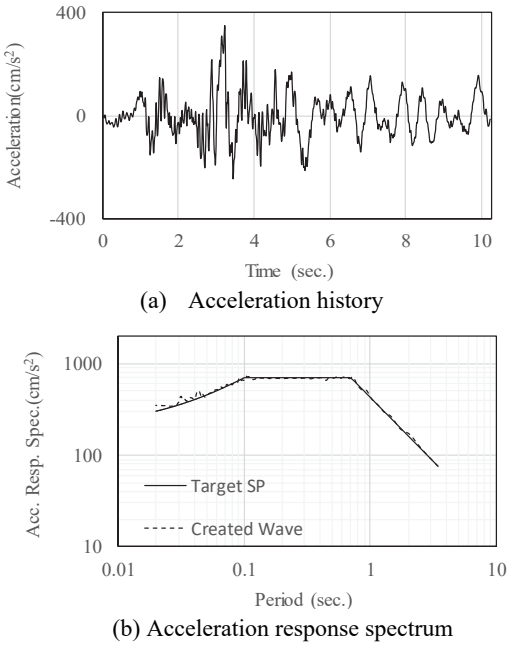

(a) Acceleration history

(b) Acceleration response spectrum

Fig. 11 Ground motion at the dam base during Earthquake B (the component perpendicular to the dam axis).

damping is thought to increase with the decrease in the material rigidity. Because the quantitative variation is unknown, the values shown in **Table 3** and Equation (2) are used to obtain a conservative evaluation.

A notable issue is the setting of the ground motion at the dam base during Earthquake B. It is assumed that a potential fault exists directly under the dam, causing an M_j 6.5 earthquake. The three-directional ground motions at the dam base are created by fitting the acceleration records of a past earthquake to the lower limit response spectra specified in the current guidelines[6]. Earthquake records at the dam base in the aftershock that occurred 62 h after the Iwate-Miyagi Nairiku Earthquake in 2008 are considered. **Figure 11** shows the created acceleration waveform and acceleration response spectrum of the component in the direction perpendicular to the dam axis as an example. The input ground motions at the bottom of the foundation rock model are created by performing the 3D inverse analysis using the ground motions defined at the dam base.

Figure 12 shows the acceleration response histories at the dam crest (T) to Earthquake B. The acceleration amplification factor is only 0.77, which is an abnormal value for a rockfill dam that is 74.4 m high and constructed using modern construction technologies. **Figure 13** shows the Fourier spectra of the acceleration responses at the crest. The acceleration responses at the crest have nearly no frequency components of 3 Hz or higher. The high-frequency components cannot propagate in the dam body since

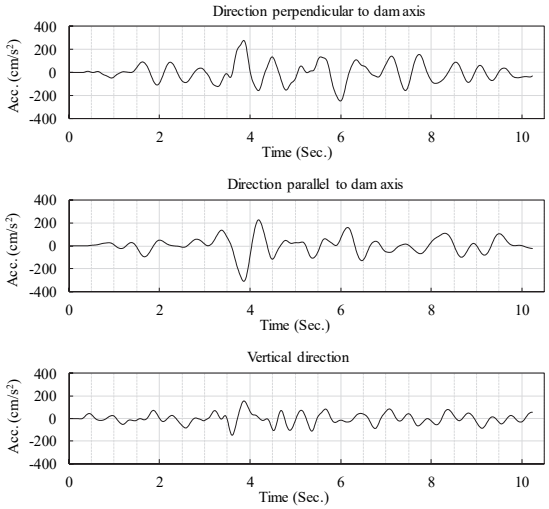

Fig. 12 Acceleration responses of the crest to Earthquake B.

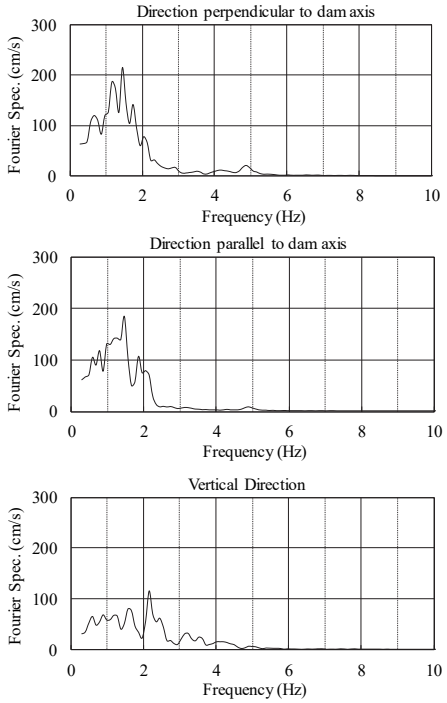

Fig. 13 Fourier spectra of acceleration response at the crest.

the rigidities of the embankment materials decreased due to Earthquake A. In Earthquake B, the rigidities of the embankment materials further decreased. The shear strains generated in the rock zones during Earthquake B range from 0.02%–1.0%. As the shear moduli of the rock materials decrease, the damping ratio increases. This aspect also explains the extremely small value of the acceleration amplification of the dam.

(2) Residual deformation caused by Earthquake B

Using the abovementioned analysis results, the residual deformation of the Aratozawa dam caused by Earthquake B is calculated using the same methods as those applied for Earthquake A. The deformation due to sliding and that related to the shaking and rearrangement of soil particles are calculated separately. Next, the vertical components of the two kinds of deformation are summed to find the maximum possible subsidence of the dam caused by Earthquake B.

Although slippage did not occur due to Earthquake A, the dam was heavily loaded, and the stiffness of the embankment materials was considerably reduced. Therefore, the use of the decreased strength of the embankment materials was considered in the calculation of the sliding deformation due to Earthquake B. To set the strength parameters, the results of past experimental studies were applied. After Tatsuoka et al.[16], a higher density corresponds to a greater decrease in the strength (internal friction angle), as indicated by the plane strain compression test. The strength is affected by the anisotropy of the specimens and reduced at most by approximately 20% at 10% of the axial strain. Sasaki et al.[17] investigated the strength and deformation properties of coarse-grained materials by performing cyclic and monotonic loading triaxial compression tests under various conditions. The static peak strength after cyclic loading reduced by approximately 20%. According to the results of the large-scale triaxial tests with quartz andesite[18], which are similar to the construction materials of the Aratozawa dam, the deviator stress reduced by 30% compared to the peak stress. In this work, considering the variability of the experimental results and to perform a conservative evaluation, the ratio of the declined strength to the peak strength is set as 2/3. The cohesion is set as zero, and the frictional angles are two-thirds their peak values. Moreover, similar to the stiffness of the dam, it is presumed that the decrease in strength likely recovered one week after the mainshock.

The calculation results show that sliding mainly occurs on the downstream slope. The sliding arcs with the maximum slip displacements are extracted from each arc group and summarized in **Table 6**. The corresponding sliding arcs are shown in **Fig. 14**. Compared with the results on the upstream side, the slip displacements on the downstream side are larger. This phenomenon likely occurs owing to the difference in the upstream and downstream slope gradients and strength of the materials. The slope of the upstream and downstream surfaces of the dam is 1:2.7 and 1:2.1, respectively. In addition, as shown in **Table 5**, the frictional angles of the downstream rock zones are slightly smaller than those of the upstream side.

Arc No. 1 is small and limited to the area near the upstream toe of the dam with a displacement of 2.80 cm. Even if this type of sliding occurs, the effect on

Table 6 Results of sliding deformation for Earthquake B.

Sliding direction	Arc group	No.	Safety factor	Slip disp. (cm)	Subsidence (cm)
Upstream side	U1	1	0.384	2.80	1.99
	U2	2	0.935	0.04	0.02
	U3	3	1.279	-	-
Downstream side	D1	4	0.700	46.20	32.91
	D2	5	0.789	76.76	49.80
	D3	6	0.950	1.71	1.10

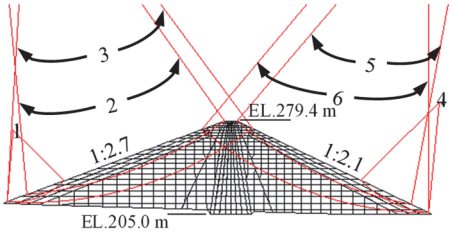

Fig. 14 Arcs with the minimum safety factor of each arc group for Earthquake B.

the stability of the dam is limited. The sliding section of arc No. 2 passes through the crest but does not reach the core, and the slip displacement is only 0.04 cm. No slippage occurs in the U3 arc group. Thus, the sliding deformations to the upstream side are judged to be permissible. Toward the downstream side, although the sliding section of arc No. 4 exhibits a displacement of 46.20 cm, the displacement is highly localized in the vicinity of the downstream toe. The sliding section of arc No. 5 passes through the crest with a sliding displacement of 76.76 cm. The subsidence at the crest accompanying the sliding reaches 49.80 cm. The sliding section of arc No. 6 cuts through the core. The maximum slip displacement is 1.71 cm, and the subsidence at the upper end of the arc is 1.10 cm.

To determine the deformation associated with the shaking and rearrangement of soil particles, the calculation process used for Earthquake A is implemented using Equation (3) and the results of the response analysis of Earthquake B. The shear moduli of the embankment materials before and after Earthquake B are considered. The results are shown in **Fig. 15**. At the crest of the dam, a maximum subsidence of 26.40 cm is predicted.

Due to the differences between the two kinds of deformation mechanisms, the deformation due to slippage cannot be simply added to the deformation related to the shaking and rearrangement of soil particles. However, in terms of the maximum potential subsidence of the dam crest, caused by Earthquake B, the vertical components calculated using the two methods can be summed to obtain a value of 76.20

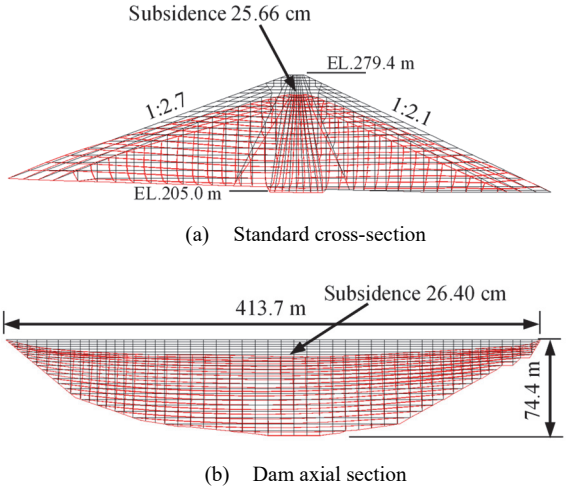

Fig. 15 Residual deformation related to the shaking and rearrangement of the soil particles caused by Earthquake B.

cm (49.80 cm + 26.40 cm) at the crest.

(3) Residual deformation caused by the doublet earthquake

The deformation caused by the doublet earthquake can be determined by summing the deformations induced by Earthquakes A and B. As the maximum possible subsidence at the dam crest, the vertical components of the two kinds of deformation can be summed directly if the location considered for each estimate is the same. Since no slippage occurred due to Earthquake A, the sliding deformation of the dam by the doublet earthquake equals that caused by Earthquake B. The maximum subsidence at the dam crest is 49.80 cm. In contrast, the deformation related to the shaking and rearrangement of the soil particles caused by the doublet earthquake can be determined by summing the deformations induced by Earthquakes A and B. It should be noted that the locations of maximum subsidence due to Earthquake A and Earthquake B are not necessarily the same. The maximum subsidence occurs at the crest with a value of 31.47 cm. Therefore, the maximum possible subsidence at the dam crest caused by the doublet earthquake is predicted to be 81.27 cm, which is the sum of the subsidence induced by sliding (49.80 cm) and shaking and rearrangement of the soil particles (31.47 cm).

The comparison of the subsidence calculated using the dam freeboard indicates that the earthquake may not induce an immediate overflow. However, the subsidence of the crest reaches a value that requires detailed investigation, for example, by performing a sequential nonlinear analysis.

(4) Seepage failure evaluation

In the calculation of the sliding deformation by

Earthquake B, arc No. 6 cuts through the core with a slip displacement of 1.71 cm. Since the elevation of the upper end of the arc is lower than the normal water level of the reservoir, it is necessary to examine the risk of seepage failure[6] (failure due to piping along the slip surface).

The risk of seepage failure is evaluated considering the hydraulic gradient calculated using Equation (4):

$$\mathrm{i} = H/L \tag{4}$$

where H is the pressure head (difference between the water level of the reservoir and elevation of the downstream end of the sliding arc in the core zone), and L is the residual length of the sliding section of the arc in the core zone. The hydraulic gradient of the sliding section of arc No. 6 in the core zone is approximately 0.91 according to Equation (4). This value is less than 1, which is generally regarded as the limit value for the occurrence of seepage failure[6] (a higher value corresponds to a more critical situation). Nevertheless, this value is relatively large; thus, a more detailed study is necessary. It is desirable to adopt appropriate precautions to prevent seepage failure.

6. PROPOSAL OF EMERGENCY MEASURES AFTER A LARGE EARTHQUAKE

Although rockfill dams constructed using modern construction techniques are unlikely to suffer from liquefaction due to a large earthquake, the occurrence of the following events must be considered:

1) Overflow due to the excessive subsidence of the crest
2) Concentrated seepage along the slip surface across the core
3) Water penetration through cracks
4) Increased seepage flow and the generation of turbid seepage water

Since these phenomena may cause dam failure, it is necessary to perform an emergency inspection immediately after a large earthquake. As clarified in this study, the seismic performance of a rockfill dam may temporarily decline due to the change in the dynamic characteristics and material properties after the occurrence of a large earthquake. Therefore, in preparation for a large earthquake that may occur later, the reservoir water should be lowered to a safe level and maintained at this level for at least a week. Moreover, before the discharge is realized, it is necessary to exchange information and coordinate with the related organizations, such as the local governments in the downstream area, and subsequently release the reservoir water according to the operation manual of the dam. Future work to respond to large-scale doublet earthquakes can be aimed at revising the dam operation manual and constructing the dam operation supporting system. Furthermore, a countermeasure must be implemented to prevent the infiltration of water into the cracks. In addition, careful monitoring of the dam body and timely analysis of the inspection records are recommended.

7. CONCLUSIONS

The following conclusions were derived through this study:

1) The relationship between the shear modulus of the embankment materials and average shear strain evaluated based on the earthquake records can be approximately expressed by a conventional hyperbolic model. When the generated average shear strain is less than approximately 2.0×10^{-4}, the stiffness of the embankment materials can be promptly recovered. However, when the shear strain exceeds 1.0×10^{-3}, the decreased stiffness requires additional time to recover. In the case of Aratozawa dam, the shear moduli of the embankment materials decreased to 58% of their original values and recovered in approximately one week.
2) The earthquake response and seismic performance of a rockfill dam subjected to a large doublet earthquake were evaluated. Moreover, a practical evaluation procedure was proposed.
3) The material properties of rockfill dams may change temporarily in response to strong seismic motion. These variations induced by the first event may significantly affect the responses of the dam to the second event. The decreased stiffness is expected to result in an increased subsidence related to the shaking and rearrangement of soil particles. The decreased strength is expected to result in an increased slip deformation.
4) To ensure dam safety immediately after a large earthquake, the reservoir water level should be rapidly reduced to a safe value and maintained at this value for at least one week in preparation for a large doublet earthquake. Careful and frequent monitoring of the dam body and timely analysis of inspection records must be ensured.

In this paper, the effect of the pore water pressure was not considered in the earthquake response analyses, and the permanent displacements of the dam

due to earthquakes were predicted using a simplified method. Future work may be aimed at using an advanced dynamic nonlinear analysis method that considers the effects of the pore water pressure.

ACKNOWLEDGMENT: We appreciate the Miyagi Prefecture Kurihara Dam Management Office and Japan Commission on Large Dams for providing us with the earthquake records and information regarding the dam considered in the present study.

REFERENCES

1) FEMA: Federal guidelines for dam safety, Earthquake analysis and design of dams, US Department of Homeland Security, 2005.
2) Matsumoto, N., Yasuda, N. and Cao, Z.: Investigation on the long-term fluctuation of the dynamic characteristics and transmitting behaviors of seismic waves in a rockfill dam – foundation system, *Journal of Structural Mechanics and Earthquake Engineering*, JSCE, No. 74 / I-3, pp. 319-329, 2018.
3) Yasuda, N., Matsumoto, N. and Cao, Z.: Study on the mechanism of the peculiar behaviors of the Aratozawa dam during the 2008 earthquake, *Journal of Disaster Research*, Vol. 13, No. 1, pp. 205-315, 2018.
4) Ohmachi, T. and Tahara, T.: Nonlinear earthquake response characteristics of a central clay rockfill dam, *Soils and Foundations*, Vol. 51, No. 2, pp. 227-238, 2011 (in Japanese).
5) JSCE Earthquake Engineering Committee: *Report on the Damage Surveys and Investigations following the 2016 Kumamoto Earthquake*, Chapter 1, Overview of the disaster area, Maruzen Publishing, 2017 (in Japanese).
6) Ministry of Land, Infrastructure, Transport and Tourism (MLIT), River Bureau: Guideline for seismic performance evaluation of dams against large earthquakes in Japan (draft), 2005 (in Japanese).
7) Yasuda, N. and Matsumoto, N.: Comparisons of deformation characteristics of rockfill materials using monotonic, cyclic loading and in-situ tests, *Canadian Geotechnical Journal*, Vol. 31, No. 2, pp. 162-174, 1994.
8) Ariga, Y., Cao, Z. and Watanabe, H.: Study on 3-D dynamic analysis of arch dam against strong earthquake motion considering discontinuous behavior of joints, *Journal of JSCE*, No. 759 / I-67, pp. 53-67, 2004 (in Japanese).
9) Miura, F. and Okinaka, H.: Dynamic analysis method for 3-D soil-structure interaction systems with the viscous boundary based on the principle of virtual work, *Journal of Structural Mechanics and Earthquake Engineering, JSCE*, No. 404 /I-11, pp. 395-404, 1989.
10) Sawada, Y. and Takahashi, T.: Study on the material properties and the earthquake behaviors of rockfill dams, *Proceedings of 4th Japan Earthquake Engineering Symposium*, pp. 695-702, 1975 (in Japanese).
11) Hatano, K., Sato, N. and Tomita, N.: Reproduction analysis of the seismic response behavior of a rockfill dam to the strong motions of the Iwate-Miyagi Nairiku Earthquake in 2008, Conference on the Technical Research of Japan Water Agency in 2010 (in Japanese).
12) Watanabe, H. and Baba, K.: A Study of sliding stability evaluation method based on the dynamic analysis of fill dams, *Large Dam*, No. 97, pp. 25-38, 1981 (in Japanese).
13) Shimamoto, K., Sato, N., Omachi, T., Kawasaki, H. and Iwai, S.: Report on damage to dams caused by the 2008 Iwate/Miyagi inland earthquake, 2008 (in Japanese).
14) Committee on the strengthening technology of Murayama dam and reservoir: Murayama reservoir maintenance committee report, 2002 (in Japanese).
15) Railway Technical Research Institute: *Design Standards of Railway Structures*, Maruzen Publishing, 1997 (in Japanese).
16) Tatsuoka, F., Sakamoto, M., Kawamura, T. and Fukushima, S.: Strength and deformation characteristics of sand in plane strain compression at extremely low pressures, *Soils and Foundations*, Vol. 26, No. 1, pp. 65-84, 1986
17) Sasaki, T., Shimamine, T., Nozawa, S., Kimura, M., Hasegawa, H., Tatsuoka, F. and Hirakawa, D.: The strength and deformation properties of coarse-grained materials from cyclic and monotonic loading triaxial compression tests under various conditions, *Journal of JSCE, Division C*, Vol. 64, No. 2, pp. 209-225, 2008 (in Japanese).
18) Hojo, K., Harita, K. and Ogawa, M.: Large-scale tri-axial test for the characteristics of fill dam materials (Shichigasyuku Dam), Technical memorandum of PWRI, No. 1507, Public Works Research Institute, Ministry of Construction, 1979 (in Japanese).

(Received December 7, 2020)
(Accepted May 22, 2021)